

# Adaptive Finite Time Intercept Guidance

Anthony J. Calise\*

Georgia Institute of Technology, Atlanta, Georgia 30332

<https://doi.org/10.2514/1.G007664>

**This paper summarizes several key issues of importance related to intercept of high-speed maneuvering targets under stratospheric altitude conditions, where it is unlikely that the interceptor will have a significant speed and/or maneuverability advantage. It explains why one cannot rely on traditional proportional navigation guidance and presents simulation results for a recently developed finite time method of guidance. A simplified version of finite time intercept guidance is derived, and a modification required to allow it to be practically implemented is described. Simulation results are presented to illustrate the advantages of the simplified version.**

## Nomenclature

$A_M$	=	missile acceleration normal to $V_T$
$A_T$	=	target acceleration normal to $V_M$
$A_{T,q}$	=	target acceleration normal to the line-of-sight
$A_{T,R}$	=	target acceleration along the line-of-sight
$g$	=	acceleration due to gravity
$N$	=	navigation gain
$q$	=	line-of-sight angle
$R$	=	range
$V_M$	=	missile velocity vector
$V_q$	=	relative velocity normal to the line-of-sight
$V_R$	=	relative velocity along the line of sight
$V_T$	=	target velocity vector
$\phi_M$	=	missile heading
$\phi_T$	=	target heading

## I. Introduction

**P**ROPORTIONAL navigation guidance (PNG) has long been the guidance approach of choice for both ground launched and air-launched guided missiles. This amounts to commanding a turn rate proportional to the instantaneous line-of-sight (LOS) rate. This is equivalent to commanding an acceleration normal to the LOS proportional to the product of range rate and LOS rate. Achieving small miss distance for finite time engagements requires that the interceptor has a sufficiently high speed and maneuver advantage. Other factors such as evasive target maneuvers, lag in following guidance commands, sensor noise, bore-sight error, and seeker dynamics also come into play. The impact of these issues and others for conventional missiles operating at normal airspeeds is addressed in Ref. [1].

In scenarios calling for intercept of high-velocity maneuvering targets at extremely high altitudes, some of the conditions normally needed for guaranteeing a small miss distance may not exist. At the most elementary level, it can easily happen that missile speed is the same or only moderately higher than target speed. Intercept can only be assured using a guidance law capable of reducing the LOS rate to zero in finite time. Such guidance laws have recently been described in Refs. [2,3]. However, these references have not addressed what happens in the nonideal case when there is a lag in following the guidance command and there are limits on the achievable acceleration, as well as other factors such as time-varying evasive target maneuvers and the effect of sensor noise in a high-gain or adaptive

setting. Methods for treating control limits, sensor noise, and unmodeled dynamic effects in adaptive systems have been developed in the case of model reference adaptive control in Refs. [4–6], but these are not “finite time” adaptive controllers.

Even the simplest mechanization of PNG requires estimation of the LOS rate because seekers and ground tracking radars provide only a direct measure of the LOS angle. Augmented forms of PNG require estimation of target acceleration. Estimation can be done by implementing a Kalman filter as detailed in Chapter 9 of Ref. [1]. Kalman filter design entails the use of a model for the behavior of the target. For example, the most common assumption is that the target acceleration is a first-order Markov process. If, on the other hand, it is known that the target is weaving, then the filter design can be optimized for a weaving target. But if the target behaves differently, then degraded performance in comparison to PN guidance can be the outcome, particularly if the estimate of time-to-go is inaccurate. It is the perspective of this author that achieving a design that is highly responsive to target maneuvers, regardless of how the target behaves, ultimately will require some form of adaptation.

In this paper a simplified version of finite time intercept guidance is derived, and a modification required to allow it to be practically implemented is described. Simulation results are presented to illustrate the advantages of the simplified version in the presence of missile response lag, acceleration limits, and evasive target maneuvers.

## II. Background

A typical missile–target engagement geometry is shown in Fig. 1, where  $V_M$  is the missile velocity and  $V_T$  is the target velocity. For constant-velocity missile and target engagements, and nonaccelerating targets, PNG ensures that miss distance asymptotically goes to zero as the initial engagement range  $R$  approaches infinity.

For the planar engagement shown in Fig. 1, the equations of motion are

$$\dot{R} = V_R \quad (1a)$$

$$\dot{V}_R = \frac{V_q^2}{R} + A_{T,R} - \sin(q - \phi_M)A_M \quad (1b)$$

$$\dot{q} = \frac{V_q}{R} \quad (1c)$$

$$\dot{V}_q = -\frac{V_q V_R}{R} + A_{T,q} - \cos(q - \phi_M)A_M \quad (1d)$$

where  $R$  is range,  $q$  is the LOS angle,  $V_q = R\dot{q}$  is the relative velocity normal to the LOS,  $\phi_M$  and  $\phi_T$  are the missile and target flight path angles,  $A_{T,R}$  and  $A_{T,q}$  are the components of target acceleration ( $A_T$ ) along and orthogonal to the LOS, and  $A_M$  is the missile acceleration. Both  $A_T$  and  $A_M$  are assumed to act perpendicular, respectively, to vectors  $V_T$  and  $V_M$ .

Presented as Paper 2023-1050 at the AIAA SciTech Forum, National Harbor, MD, January 23–27, 2023; received 8 February 2023; accepted for publication 16 April 2023; published online 12 May 2023. Copyright © 2023 by the Emeritus Professor, School of Aerospace Engr., Georgia Tech. Published by the American Institute of Aeronautics and Astronautics, Inc., with permission. All requests for copying and permission to reprint should be submitted to CCC at [www.copyright.com](http://www.copyright.com); employ the eISSN 1533-3884 to initiate your request. See also AIAA Rights and Permissions [www.aiaa.org/randp](http://www.aiaa.org/randp).

\*Emeritus Professor, School of Aerospace Engineering; [acalise@ae.gatech.edu](mailto:acalise@ae.gatech.edu). Fellow AIAA.

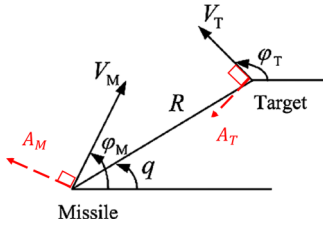


Fig. 1 Missile-target engagement geometry.

In this section a computer simulation based on the intercept dynamics described in Eqs. (1a–1d) is used to first reproduce the results in Ref. [3], and then to evaluate the effects of missile response lag and acceleration limit. Three guidance laws are compared. The first is the one developed by the authors of Ref. [3] called adaptive finite time nonlinear guidance (AFTNG). This is based on finite time adaptive control theory that entails proving that the candidate Lyapunov function goes to zero in finite time. The second is the guidance law developed in Ref. [2] called finite time convergence guidance (FTCG), and the third is PNG. In the case of PNG, missile acceleration command takes the well-known form

$$A_M = \frac{1}{\cos(q - \phi_M)} (-NV_q V_r / R) \quad (2)$$

where  $N$  is the navigation gain. In the FTCTG law of Ref. [2] we have

$$A_M = \frac{1}{\cos(q - \phi_M)} \left( -NV_q V_r / R + f * \min\{1, \dot{q}/\varepsilon\} + c * |\dot{q}|^\eta * \text{sign}(\dot{q}) \right) \quad (3)$$

where the parameter  $f > 0$  represents a bound on target acceleration and both  $c$  and  $\eta$  are positive guidance parameters. Its derivation relies on finite time Lyapunov stability theory. In Ref. [2] the parameters in Eq. (3) were chosen as  $f = 25 \text{ m/s}^2$ ,  $c = 30$ ,  $\varepsilon = 0.005$ , and  $\eta = 0.4$ . The AFTNG law of Ref. [3] is also derived using finite time Lyapunov stability theory, and has the following form:

$$A_M = \frac{1}{\cos(q - \phi_M)} (-V_q V_r / R + k_1 V_q |V_q|^{-\gamma} + k_2 \xi_1 + k_3 \xi_2) \quad (4a)$$

in which  $\xi_1$  and  $\xi_2$  are adaptation states defined by

$$\dot{\xi}_1 = \frac{V_q}{|V_q|}, \quad \dot{\xi}_2 = k_2 k_3 |\xi_2| \frac{V_q}{|V_q|} - k_4 \frac{\xi_2}{|\xi_2|} \quad (4b)$$

The parameter values were chosen as follows:  $k_1 = 3$ ,  $k_2 = 2$ ,  $k_3 = 0.01$ ,  $k_4 = 30$ , and  $\gamma = 0.5$ . Note that the leading terms in both the FTCTG law and the AFTNG laws have the same form as the PNG law. The AFTNG law of Ref. [3] amounts to setting  $N = 1$ , and in all the comparisons done there to both the FTCTG law and the PNG law,  $N = 3$  was used for the FTCTG law and  $N = 4$  was used for the PNG law. In the remainder of this section the same parameter settings are used.

#### A. Scenario 1 in Ref. [3]

With reference to Fig. 1, both the target and missile are modeled as flying at constant velocity with  $V_T = 700 \text{ m/s}$  and  $V_M = 800 \text{ m/s}$ , and having initial conditions  $\phi_M(0) = 5^\circ$ ,  $\phi_T(0) = 150^\circ$ ,  $R(0) = 40,000 \text{ m}$ . The target is accelerating at  $A_T = -25 \text{ m/s}^2$  ( $2.55g$ ) throughout the engagement. The resulting target and missile trajectories for the three guidance laws are shown in Fig. 2a. The simulations are terminated when either the estimated time-to-go falls below the integration step size, or closing velocity becomes positive. Both the FTCTG and the AFTNG laws result in a near-zero miss distance, with FTCTG intercept occurring later in time. The PNG

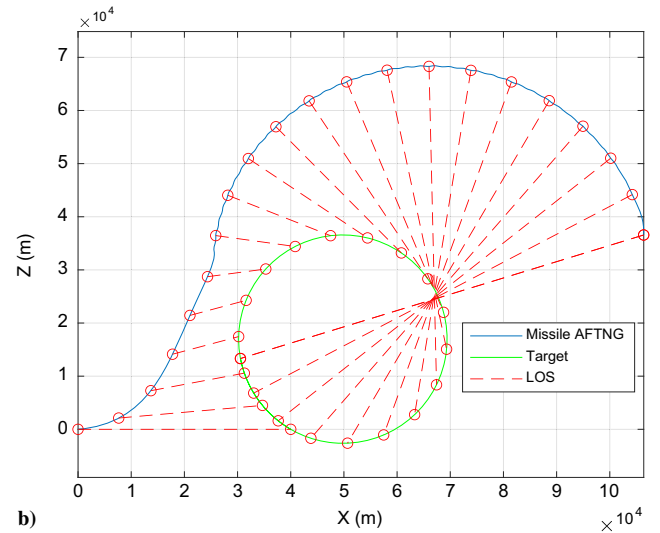
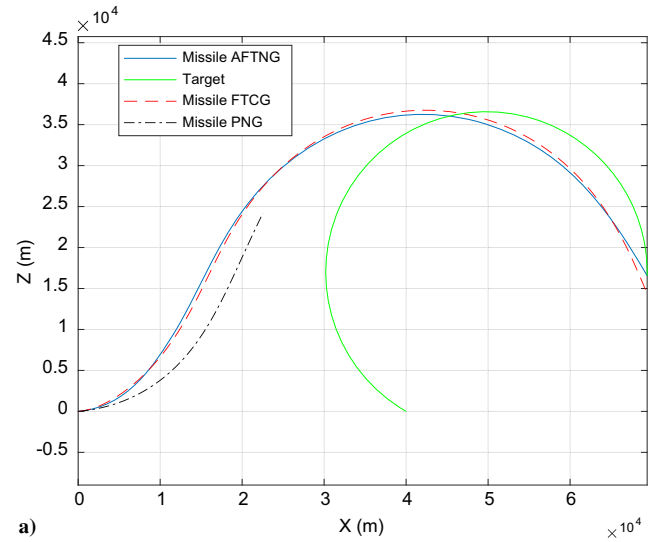


Fig. 2 a) Missile and target trajectories. b) The 200 s PNG missile and target engagement profile.

trajectory is terminated very early due to closing velocity becoming positive. The results shown in Fig. 2a are identical to what is shown in Fig. 8 of Ref. [3]. The PNG guided trajectory flown beyond the point where the closing velocity becomes positive is shown Fig. 2b, over a period of 200 s. This figure also shows the LOS at 10 s intervals. The corresponding history of LOS rate for all three cases is shown in Fig. 3, which agrees with the results shown in Fig. 7 of Ref. [3]. The FTCTG law does not reduce the LOS rate to zero before intercept. It is guaranteed to do so only for nonmaneuvering targets. On the other hand, the AFTNG law does reduce the LOS rate to zero before intercept because of the action of the two adaptive terms in Eq. (4a). Figure 4 shows the manner in which the relative velocity normal to the LOS (relative lateral velocity) is reduced to zero in finite time by the AFTNG law. Figure 5 compares the acceleration profiles for the three guidance laws. The acceleration profiles for the AFTNG and FTCTG are similar. The command using FTCTG becomes very large at the end due to the small but finite miss distance. Figure 6 demonstrates the action of the sum of the two AFTNG adaptive terms in canceling the component of target acceleration normal to the LOS. This is why the AFTNG is successful in achieving and maintaining finite time guidance (reducing relative lateral velocity and LOS rate to zero in finite time before intercept) even in the presence of target accelerations.

*Comment 2.1:* In Ref. [3] the second adaptation state  $\xi_2$  in Eq. (4b) was given a nonzero initial value, which is not commonly done in adaptive control. If the initial value is set to zero, then it is apparent

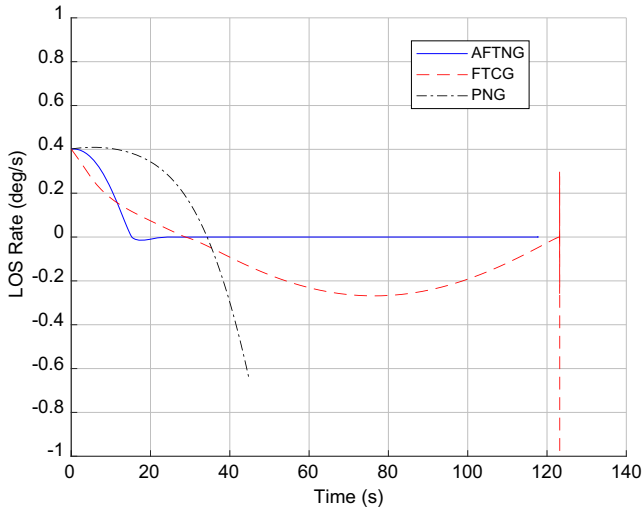


Fig. 3 LOS rate profiles.

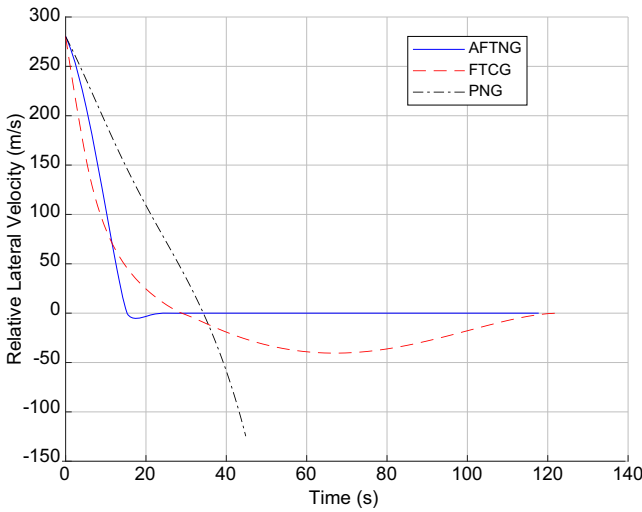


Fig. 4 Relative lateral velocity profiles.

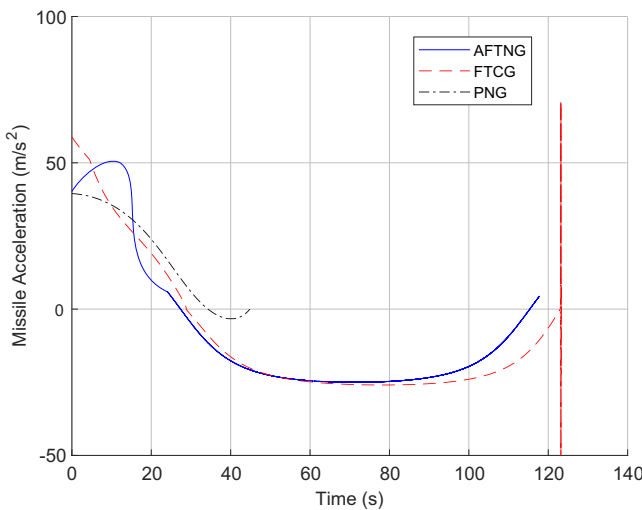


Fig. 5 Missile acceleration profiles.

from Eq. (4b) that  $\xi_2(t) = 0$ . The value used can be seen in Fig. 6 as  $\xi_2(0) = -20$ , but no mention of this fact was made in Ref. [3].

*Comment 2.2:* The proof of stability in Ref. [2] is based on the FTCTG law in Eq. (3). However, in simulation the term  $\text{sign}(\dot{q})$  is replaced with  $\text{sat}\{\dot{q}/\varepsilon\} = \min\{1, \dot{q}/\varepsilon\}$ , as defined in Eq. (44) of

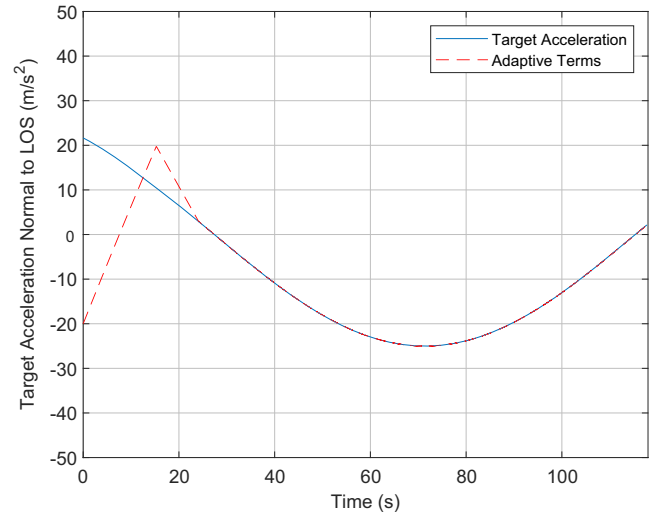


Fig. 6 Comparison of target acceleration normal to the LOS with the sum of the two adaptive terms in the AFTNG law.

Ref. [2]. Otherwise there would be chattering in the FTCTG acceleration command. This explains the FTCTG behaviors in Figs. 3 and 5 above at the very end of the intercept.

*Comment 2.3:* The parameter  $k_4$  in Eq. (4b) of the AFTNG law is assumed to depend on  $|\xi_1(t)|$  in the stability proof in Ref. [3], and therefore should be implemented as  $k_4(t)$ . However, it is listed in Table 1 of Ref. [3] as  $k_4 = 30$ , and the parameters needed to properly implement  $k_4(t)$  are not provided. Therefore the AFTNG results shown above are all with  $k_4 = 30$ , and the implied assumption is that  $k_4(t) < 30$ .

## B. Effect of Missile Response Lag and Acceleration Limits

The effects of missile response lag and acceleration limits were not addressed in Refs. [2,3]. In this section we consider these effects by imposing a 5g limit and second-order filtering of the missile acceleration command (to represent missile response lag). The filter has a natural frequency of 2 rad/s and a damping ratio of 0.7. Figure 7 shows the resulting effect on AFTNG missile acceleration. This should be compared with the AFTNG response in Fig. 5. Figure 8 shows the effect this has on the ability of the sum of the two adaptive terms in canceling the target acceleration normal to the LOS. This should be compared with the response in Fig. 6. The resulting miss distance is 3.9 m (not shown).

Figure 9 shows what happens to the same engagement when a  $G$  limit = 1.3 times the target acceleration is imposed on the command,

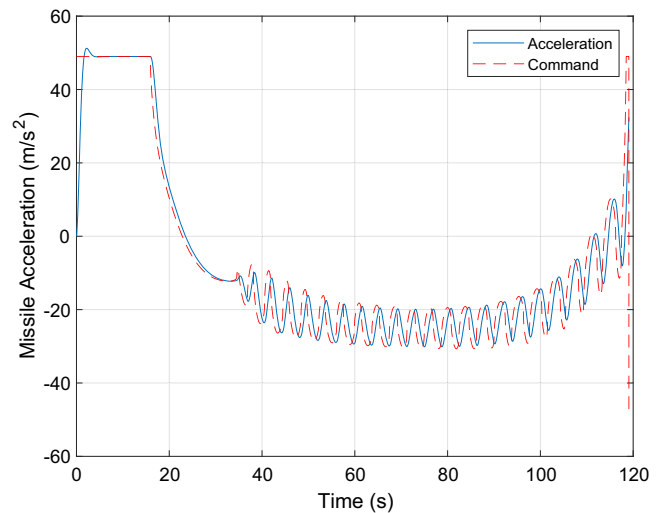


Fig. 7 AFTNG acceleration with lag and a 5g command limit.

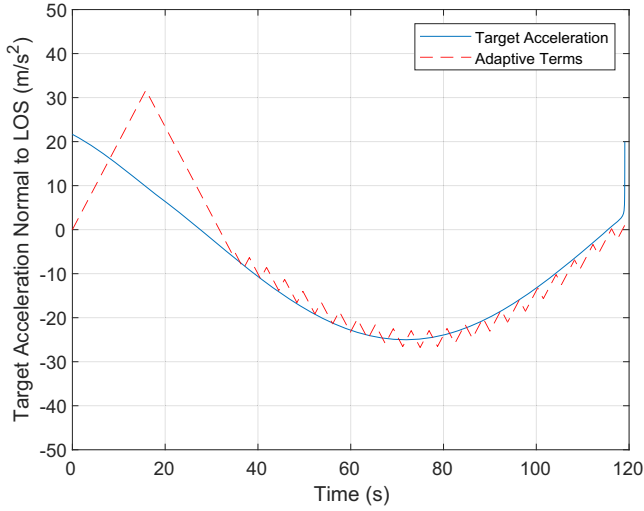


Fig. 8 The effect of lag on AFTNG adaptation.

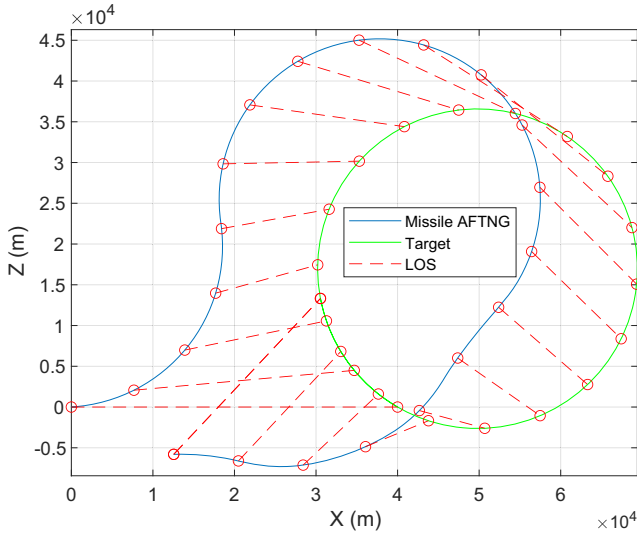


Fig. 9 The 200 s AFTNG missile and target engagement profile with missile lag and  $G$  limit =  $1.3 * A_T$ .

or a  $3.32g$  limit. This shows that acceleration advantage has a dramatic effect on miss distance.

### III. Simplified Version of AFTNG

The simplified version of AFTNG (S-AFTNG) presented here requires only one adaptive term. In stating the following theorem, it is assumed that both  $A_{T,q}$  and its time rate of change satisfy the following bounds:

$$|A_{T,q}| \leq L_{A_T}, \quad |\dot{A}_{T,q}| \leq L_{\dot{A}_T} \quad (5)$$

*Theorem:* The guidance law

$$\begin{cases} A_M = \frac{1}{\cos(q - \phi_M)} \left( -\frac{V_q V_R}{R} + k_o(t) + \xi \right) \\ \dot{\xi} = k_1 \text{sign}(V_q), \quad k_1 > 0 \end{cases} \quad (6a)$$

with

$$k_o(t) = [L_{\dot{A}_T}(L_{A_T} + |\xi|) + \eta] * \text{sign}(\dot{q})/k_1, \quad \eta > 0 \quad (6b)$$

ensures both  $V_q$  and  $(A_{T,q} - \xi)$  go to zero in finite time.

*Proof:* Consider the Lyapunov function candidate

$$V = k_1 |V_q| + (A_{T,q} - \xi)^2 / 2 \quad (7)$$

Then

$$\dot{V} = k_1 \text{sign}(V_q) \dot{V}_q + (A_{T,q} - \xi) * [\dot{A}_{T,q} - k_1 \text{sign}(\dot{q})] \quad (8)$$

Using the first of Eq. (6a) in Eq. (1d) results in

$$\dot{V}_q = A_{T,q} - k_o(t) + \xi \quad (9)$$

Substituting Eq. (9) in Eq. (8), and noting that that  $\text{sign}(V_q) = \text{sign}(\dot{q})$ , then canceling like terms involving  $\text{sign}(\dot{q})$ , it follows that

$$\dot{V} = -k_1 k_o(t) \text{sign}(\dot{q}) + \dot{A}_{T,q} (A_{T,q} - \xi) \quad (10)$$

Therefore  $k_o(t)$  in Eq. (6b) ensures that  $\dot{V} < \eta$ , which in turn implies that both  $V_q$  and  $(A_{T,q} - \xi)$  go to zero in finite time.

*Comment 3.1:* Implementation of the guidance law in Eq. (6a) assumes that the missile seeker is capable of accurately measuring  $q$ ,  $\dot{q}$ , and  $R$ , which is also the case for AFTNG, FTNG, and PNG. Moreover, since  $V_q = \dot{q} * R$ , the theorem also implies that the LOS rate goes to zero in finite time.

*Comment 3.2:* The first term in Eq. (6a) corresponds to the PNG law with a navigation gain of  $N = 1.0$ .

*Comment 3.3:* Even if  $A_T$  is constant,  $\dot{A}_{T,q}$  in general is not zero because it depends on the time rate of change of both  $q$  and  $\phi_T$ .

*Comment 3.4:* The most important difference between S-AFTNG and the AFTNG law of Ref. [3] is the appearance of  $\text{sign}(\dot{q})$  in Eq. (6b), which directly affects the guidance law in Eq. (6a), whereas it only appears indirectly in the AFTNG adaptation laws. This issue, which (as explained in *Comment 2.2*) also arises in the FTNG law of Ref. [2], is addressed in the next section.

### IV. S-AFTNG Performance Evaluation

This section presents an evaluation of the S-AFTNG law when subjected to an acceleration command limit, missile response lag, and a sinusoidal evasive target maneuver. Similar to the FTNG law of Ref. [2], practical implementation requires some form of modification be applied to prevent chattering in the guidance command due to the presence of  $\text{sign}(\dot{q})$  in Eq. (6b). In what follows,  $\text{sign}(\dot{q})$  is replaced by the sigmoidal form

$$\text{sig}(\dot{q}) = (e^{\alpha \dot{q}} - 1) / (e^{\alpha \dot{q}} + 1), \quad \alpha > 0 \quad (11)$$

The parameter  $\alpha$  in Eq. (11) is regarded as providing a compromise between achieving the ideal in reducing  $\dot{q}$  to zero in finite time, and imposing a reasonable demand in missile's ability to respond to the guidance command. Figure 10 illustrates the behavior of  $\text{sig}(\dot{q})$  for several values of  $\alpha$ .

The parameter settings (in mks units) chosen for the S-AFTNG guidance law in Eqs. (6a) and (6b) are as follows:

$$k_1 = 1, \quad L_{A_T} = 50, \quad L_{\dot{A}_T} = 25, \quad \eta = 10, \quad \alpha = 5 \quad (12)$$

We first consider the same  $-25 \text{ m/s}^2$  target maneuver as in the previous section, with missile  $G$  limit = 5, and the same lag modeling of missile response. Figure 11a shows the missile acceleration profile. The command limit is not encountered except at intercept. Figure 11b shows the behavior of the adaptive term  $\xi(t)$  in estimating  $A_{T,q}$ . These figures should be compared with the AFTNG responses shown in Figs. 7 and 8. Figure 11c shows that the LOS rate is driven to near zero in approximately 60 s. The corresponding time history of the Lyapunov candidate is shown in Fig. 11d. The resulting miss distance is essentially zero.

Recall that the AFTNG law of Ref. [3] fails to intercept a constant maneuvering target with missile lag and acceleration limit set at or below 1.3 times the target acceleration (see Fig. 9). Figure 12 shows

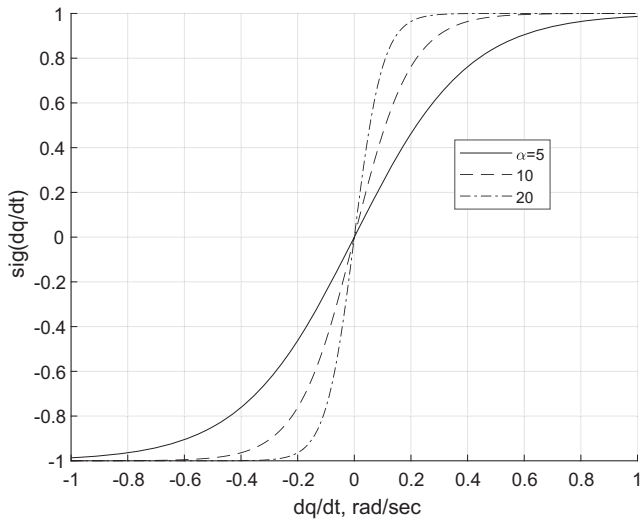


Fig. 10 The  $\text{sig}(\dot{q})$  for several values of  $\alpha$ .

that the S-AFTNG law is able to intercept the same target with missile lag and acceleration limit reduced to 1.1 times the target acceleration. The miss distance in this case is close to zero.

Finally we examine what happens when the target superimposes a  $-10 \text{ m/s}^2$  sinusoidal weave with a natural frequency of 1 rad/s on top

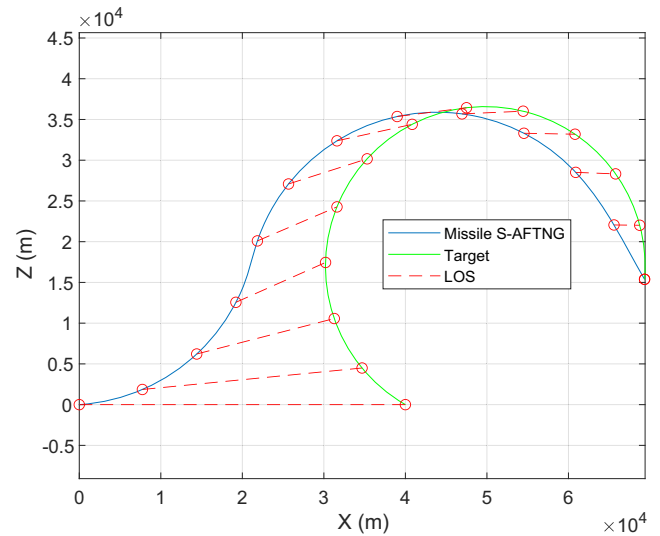
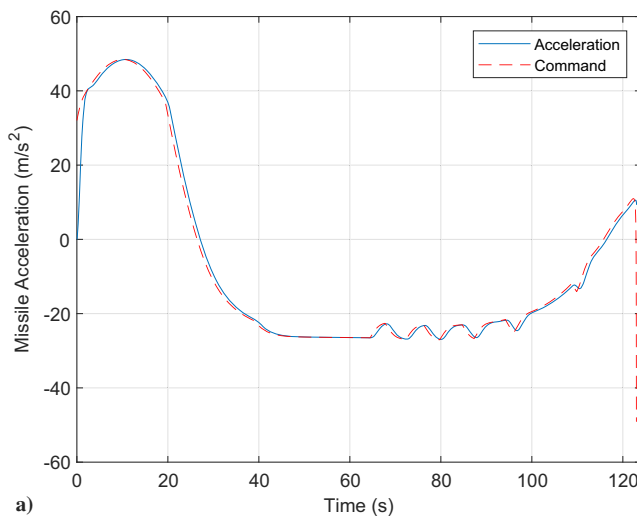
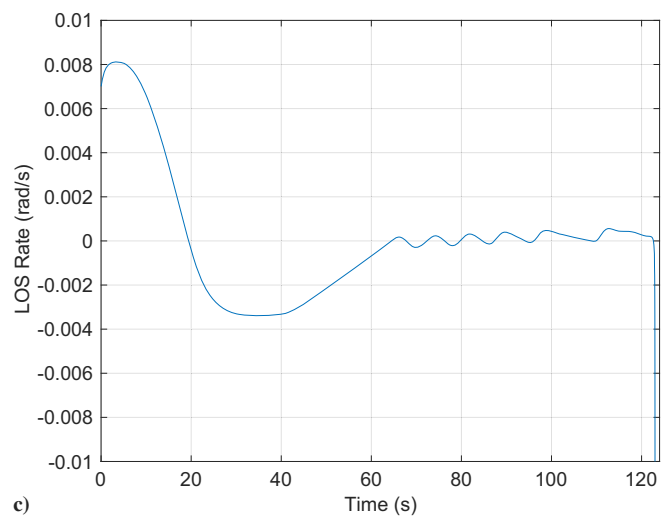


Fig. 12 The S-AFTNG engagement of a maneuvering target with missile lag and  $G \text{ limit} = 1.1 * A_T$ .

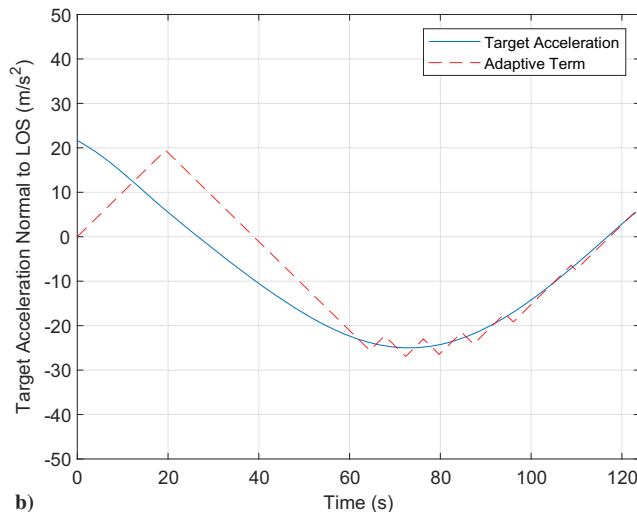
of the  $-25 \text{ m/s}^2$  constant maneuver, and with missile lag and 3g limit. The 3g limit is equivalent to approximately 1.18 times the constant portion of the target maneuver, and 0.84 times the peak in the target acceleration. In Ref. [1], it is shown that a weaving maneuver at



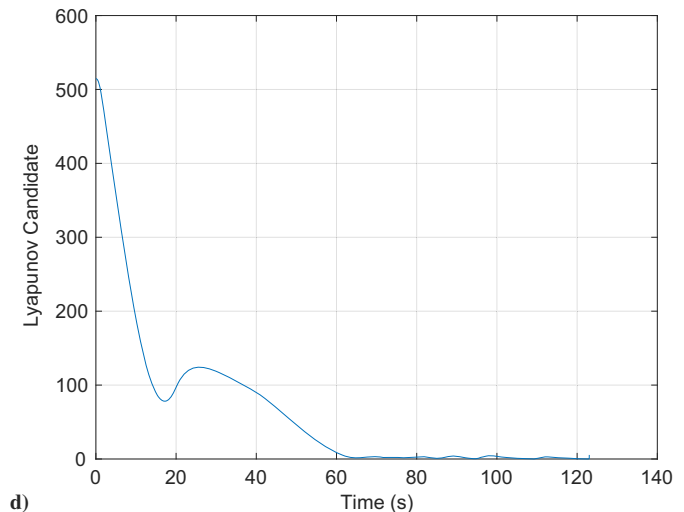
a)



c)



b)



d)

Fig. 11 a) S-AFTNG acceleration with lag and 5g command limit. b) The effect of lag on S-AFTNG adaptation. c) S-AFTNG LOS rate with lag and 5g command limit. d) S-AFTNG Lyapunov candidate with lag and 5g command limit.



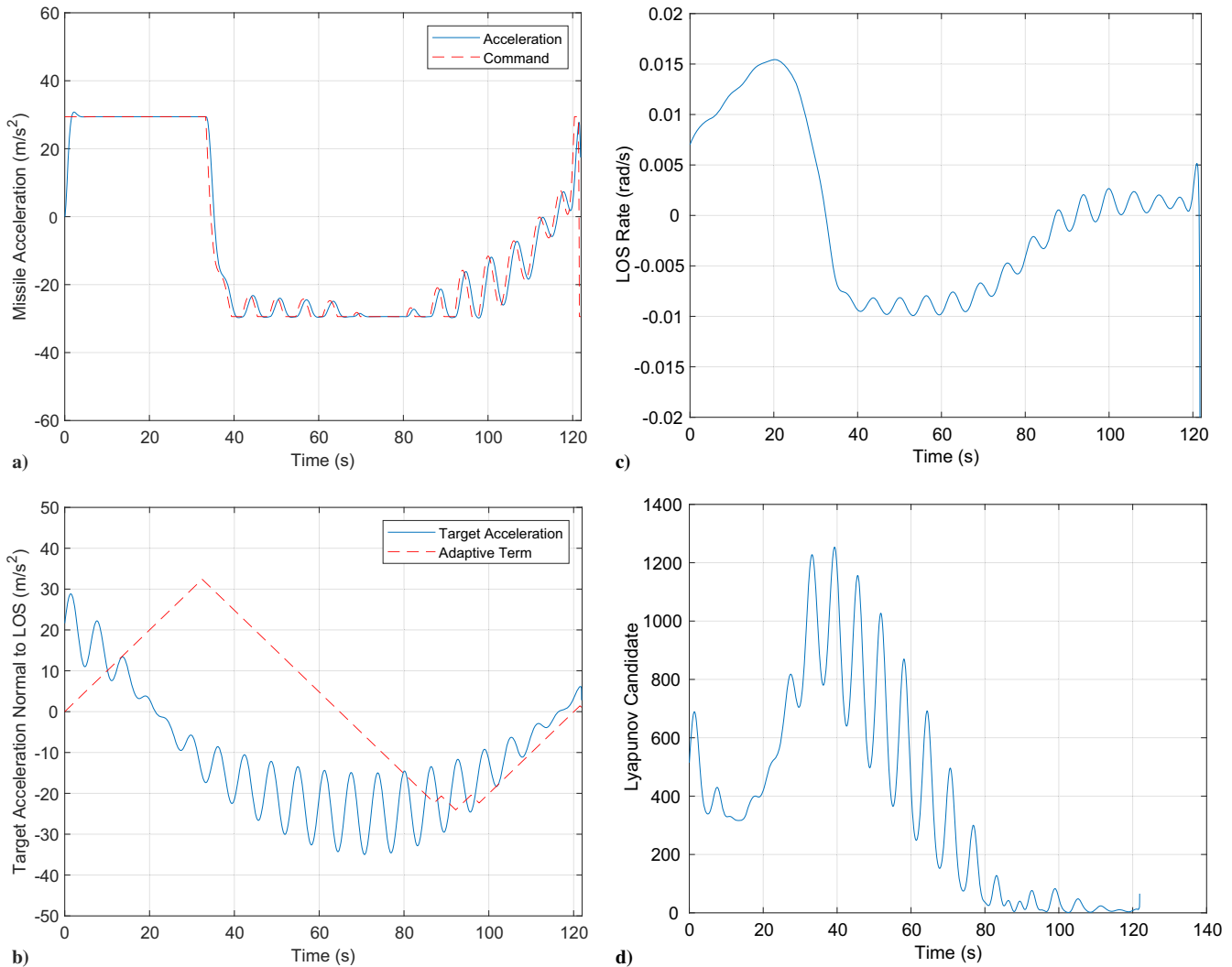


**Fig. 13** a) Missile acceleration profile for a weaving target. b) Comparison of  $A_{T,q}$  and  $\xi(t)$  for a weaving target. c) LOS rate for a weaving target. d) Lyapunov candidate for a weaving target.

this frequency tends to maximize miss distance in the case of PNG guidance. Figures 13a–13d show the corresponding S-AFTNG results for this case. The miss distance in this case is 0.57 m. The AFTNG law misses the target by a large amount, and the resulting engagement profile is similar to that shown in Fig. 9.

## V. Conclusions

The most significant factors concerning the problem of intercepting high-velocity targets at stratospheric altitudes are the ability of the missile to have a sufficient speed and maneuver advantage. PNG guidance requires at least a 2-to-1 speed and maneuver advantage. It is highly likely that a finite time form of guidance will be needed if these levels of advantage are not present. AFTNG is clearly superior to FTNG guidance in the absence of missile response lag and acceleration limit. However, adaptive guidance methods are more vulnerable to unmodeled effects, and a more robust adaptive approach will be needed. One means of achieving the required robustness is to modify the presented simplified AFTNG guidance command to enable a compromise between the ideal of driving the LOS rate to zero in finite time and the ability to maintain performance in the presence of non-ideal conditions, such as sensor noise, missile response lag, and target evasive maneuvering.

## References

- [1] Zarchan, P., *Tactical and Strategic Missile Guidance*, 4th ed., Progress in Astronautics and Aeronautics, AIAA, Reston, VA, 2002, Chap. 6.  
<https://doi.org/10.2514/4.868948>
- [2] Zhou, D., and Sun, S., "Guidance Laws with Finite Time Convergence," *Journal of Guidance, Control, and Dynamics*, Vol. 32, No. 6, 2009, pp. 1838–1846.  
<https://doi.org/10.2514/1.42976>
- [3] Behnamgol, V., Vali, A., and Mohammadi, A., "A New Adaptive Finite Time Nonlinear Guidance Law to Intercept Maneuvering Targets," *Aerospace Science and Technology*, Vol. 68, Sept. 2017, pp. 426–421.  
<https://doi.org/10.1016/J.AST.2017.05.033>
- [4] Johnson, E., and Calise, A. J., "Neural Network Adaptive Control of Systems with Input Saturation," *American Control Conference*, Inst. of Electrical and Electronics Engineers, New York, June 2001, pp. 3527–3532.  
<https://doi.org/10.1109/ACC.2001.946179>
- [5] Yucelen, T., and Calise, A. J., "Robustness of a Derivative-Free Adaptive Control Law," *Journal of Guidance, Control, and Dynamics*, Vol. 37, No. 5, Sept.–Oct. 2014, pp. 1583–1594.  
<https://doi.org/10.2514/1.G000289>
- [6] Chandramohan, R., and Calise, A. J., "Output Feedback Adaptive Control of Plants with Unmodeled Dynamics and Input Uncertainties," *Journal of Guidance, Control, and Dynamics*, Vol. 42, No. 10, Oct. 2019, pp. 2143–2156.  
<https://doi.org/10.2514/1.G003548>